

## Effects of high oxygen tension on healthy volunteer microcirculation

Nicolas Cousin<sup>1</sup>, Julien Goutay<sup>1</sup>, Patrick Girardie<sup>1</sup>, Raphaël Favory<sup>1</sup>, Elodie Drumez<sup>2</sup>, Daniel Mathieu<sup>1</sup>, Julien Poissy<sup>1</sup>, Erika Parmentier<sup>1</sup>, Thibault Duburcq<sup>1</sup>

<sup>1</sup> Pôle de réanimation, hôpital Roger Salengro, CHU Lille, Lille, France

<sup>2</sup> Unité de méthodologie – biostatistique et data management, CHU Lille, Lille, France

**Corresponding author:** Dr Thibault Duburcq, Centre Hospitalier Universitaire de Lille, Hôpital Roger Salengro – Centre de réanimation, Avenue du Professeur Emile Laine, 59037 LILLE Cedex, France

[thibault.duburcq@chru-lille.fr](mailto:thibault.duburcq@chru-lille.fr)

### Keywords

Hyperbaric oxygen treatment; Hyperoxia; Laser Doppler flowmetry; Near-infrared spectroscopy; Perfusion

### Abstract

(Cousin N, Goutay J, Girardie P, Favory R, Drumez E, Mathieu D, Poissy J, Parmentier E, Duburcq. Effects of high oxygen tension on healthy volunteer microcirculation. *Diving and Hyperbaric Medicine*. 2022 December 20;52(4):260–270. doi: [10.28920/dhm52.4.260-270](https://doi.org/10.28920/dhm52.4.260-270). PMID: 36525683.)

**Introduction:** Previous studies have highlighted hyperoxia-induced microcirculation modifications, but few have focused on hyperbaric oxygen (HBO) effects. Our primary objective was to explore hyperbaric hyperoxia effects on the microcirculation of healthy volunteers and investigate whether these modifications are adaptative or not.

**Methods:** This single centre, open-label study included 15 healthy volunteers. Measurements were performed under five conditions: T0) baseline value (normobaric normoxia); T1) hyperbaric normoxia; T2) hyperbaric hyperoxia; T3) normobaric hyperoxia; T4) return to normobaric normoxia. Microcirculatory data were gathered via laser Doppler, near-infrared spectroscopy and transcutaneous oximetry (PtcO<sub>2</sub>). Vascular-occlusion tests were performed at each step. We used transthoracic echocardiography and standard monitoring for haemodynamic investigation.

**Results:** Maximal alterations were observed under hyperbaric hyperoxia which led, in comparison with baseline, to arterial hypertension (mean arterial pressure 105 (SD 12) mmHg vs 95 (11),  $P < 0.001$ ) and bradycardia (55 (7) beats·min<sup>-1</sup> vs 66 (8),  $P < 0.001$ ) while cardiac output remained unchanged. Hyperbaric hyperoxia also led to microcirculatory vasoconstriction (rest flow 63 (74) vs 143 (73) perfusion units,  $P < 0.05$ ) in response to increased PtcO<sub>2</sub> (104.0 (45.9) kPa vs 6.3 (2.4),  $P < 0.0001$ ); and a decrease in laser Doppler parameters indicating vascular reserve (peak flow 125 (89) vs 233 (79) perfusion units,  $P < 0.05$ ). Microvascular reactivity was preserved in every condition.

**Conclusions:** Hyperoxia significantly modifies healthy volunteer microcirculation especially during HBO exposure. The rise in PtcO<sub>2</sub> promotes an adaptative vasoconstrictive response to protect cellular integrity. Microvascular reactivity remains unaltered and vascular reserve is mobilised in proportion to the extent of the ischaemic stimulus.

### Introduction

Inhalation of high oxygen concentrations is a standard therapy in many medical situations. To ensure sufficient oxygenation, supraphysiological levels are commonly used. During the nineteenth century, Paul Bert and J Lorrain Smith discovered that high oxygen tensions may lead to toxicity. Mechanisms involved include reactive oxygen species production, pulmonary oedema, altered endothelial function, activation of coagulation and reduced cardiac output. Recent meta-analyses of the potential benefits of hyperoxia in critically-ill patients have been controversial.<sup>1,2</sup> However, some subgroup analyses, supported by animal experiments, have shown a potential benefit of hyperoxia in highly selected patients (e.g., focal cerebral ischaemia).<sup>3–5</sup> Hyperbaric oxygen treatment (HBOT), where trancutaneously measured tissue oxygen partial pressure (PtcO<sub>2</sub>) is up to ten times higher than normal, has proved to be beneficial in diverse conditions.<sup>6</sup>

Microcirculatory perfusion is a key component of tissue oxygen delivery. A recent study used side-stream dark-field (SDF) imaging to provide anatomic based information on the human microcirculation in healthy volunteers exposed to normobaric (NB) hyperoxia. Its two main findings were a reversible, significant decrease in perfused microvascular density and an increased heterogeneity in microcirculatory perfusion.<sup>7</sup> Those results raised concerns about oxygen therapy safety. Indeed, microvascular alterations (impairment of nitric oxide dysregulation-induced arteriolar vasodilation, functional impairment of many cell types found in the microcirculation and increased venular leukocyte-endothelial interaction) have been independently associated with poor outcomes in critically-ill septic patients.<sup>8</sup> However, while these alterations in critically-ill patients' microcirculation resulted in tissue hypoxia (microcirculatory abnormalities contribute to a decreased functional capillary density with less perfused areas), it is not the case in healthy subjects.<sup>9–11</sup> These microvascular alterations might be an adaptive phenomenon protecting cellular integrity from a drastic

rise in oxygen partial pressure ( $PO_2$ ). The pathophysiology causing microcirculatory changes in sepsis is different than the physiologic 'adaptive' response seen with HBO.

In HBO exposure, hyperbaric (HB) hyperoxia further increases oxygen doses, thus may lead to greater microcirculation modification with a potential risk of hypoxia even in healthy subjects. Relevant data are scarce. The fact remains that HBO has been in use for over a century, and HBO-induced hypoxic injury has not been seen. One study exposed rabbits to both NB and HB hyperoxia and highlighted a significant decrease in microvascular density in both conditions.<sup>12</sup> Nevertheless, while the microcirculation may change, the significant elevation in arterial  $PO_2$  during HBOT allows for adequate  $O_2$  delivery to tissue/mitochondria despite the vasoconstriction. A recent study of HBO exposure in human subjects found that microcirculatory vasoconstriction did not inhibit the development of increased tissue oxygen partial pressure.<sup>13</sup>

Hence, to better understand the effects of hyperoxia on the microcirculation, we designed a study to explore microvascular function of healthy subjects exposed to both NB and HB hyperoxia. Our primary objective was to assess the impact of HB hyperoxia on a surrogate of microvascular function: the microvascular reactivity to an ischaemic stimulus. The other objectives were to study the impact of HB hyperoxia on healthy human microcirculatory perfusion, the impact of NB hyperoxia on microcirculatory perfusion and reactivity, and the haemodynamic response during the various oxygen exposures.

## Methods

The study received ethics (Comité de Protection des Personnes Ile de France V) and institutional (Agence Nationale de Sécurité des Médicaments et des produits de santé) approvals, and was registered on [Clinicaltrials.gov](https://clinicaltrials.gov) under NCT03980210.

This was a single centre open label study conducted in the hyperbaric oxygen facility of a teaching hospital (CHU Lille), between June and July 2019. Non-professional divers between 18 and 64 years old who had received medical clearance to practice scuba-diving in the past year were able to participate to the study. People 65 years of age and more were considered more likely to exhibit age-linked microvascular modifications, and were not included in our study. After obtaining written informed consent, inclusion criteria were checked by an independent physician from the Clinical Investigation Centre of our institution. Patients with disease known to alter microcirculation (i.e., arterial hypertension, smoking, diabetes, arteriopathy, systemic sclerosis, Raynaud's disease) or a contraindication to HBOT (e.g., heart failure, pneumothorax, unstable asthma, perilymph fistula, vestibular disorders, vascular proliferation in the eye) were excluded. General and anthropometric data such as age, gender, weight and height were recorded.

## PROTOCOL

Subjects lay on a bed inside a hyperbaric chamber throughout study and were exposed to five consecutive conditions: T0) baseline value (normobaric normoxia) with the subject breathing air at atmospheric pressure; T1) hyperbaric normoxia with a tightly fitting aviator style mask delivering a hypoxic gas mix (8% oxygen, 92% nitrogen) at 253.3 kPa (2.5 atmospheres absolute [atm abs]) ambient pressure; T2) hyperbaric hyperoxia with oxygen ( $FiO_2 = 1$ ) delivered via the same mask at 253.3 kPa ambient pressure; T3) normobaric hyperoxia with oxygen ( $FiO_2 = 1$ ) delivered via the same mask at 101.3 kPa ambient pressure; T4) a final set of measurements after return to normobaric normoxia conditions to detect residual effects of hyperoxia.

Measurements were performed after a 30-minute period in each condition to let the microcirculation and any haemodynamic changes reach an equilibrium (Figure 1).

At each step of the study protocol, vascular occlusion tests (VOTs) were performed with a cuff positioned over the brachial artery. It was inflated to at least 50 mmHg over systolic arterial pressure for 3 min as longer durations tend to compromise the subject's comfort, and shorter ones provide insufficient post-occlusive reactive hyperaemia (PORH).<sup>14</sup> On completion of the ischaemic period, the cuff was quickly deflated to zero.

Two investigators present in the hyperbaric chamber and a trained certified hyperbaric technologist ensured safety during the whole protocol.

## MEASUREMENTS

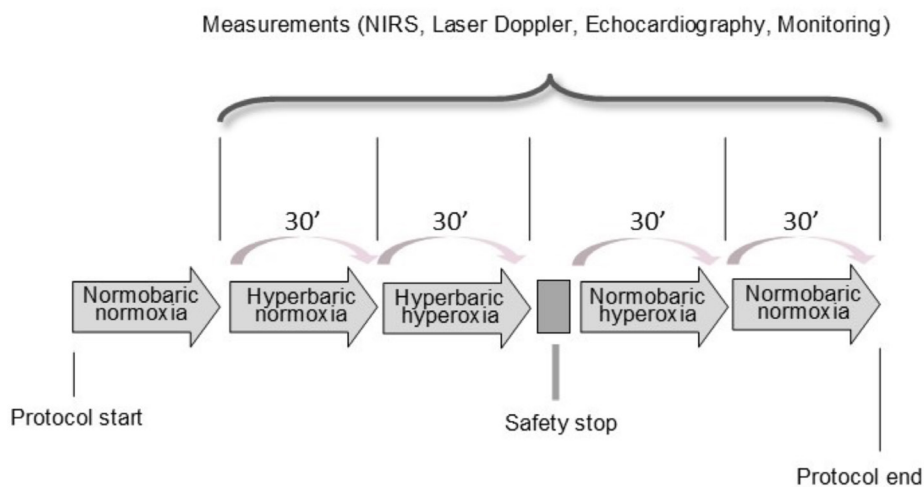
### *Microcirculatory parameters*

Subclavian artery transcutaneous pressures of  $O_2$  ( $PtcO_2$ ) and carbon dioxide ( $CO_2$ ) ( $PtcCO_2$ ) were continuously recorded (PERIFLUX® PF5040, Perimed, Jirfalla, Sweden).

Near infrared spectroscopy (NIRS) was used to detect changes in muscle perfusion. NIRS data were acquired with an INSPECTRA® 850 monitor (Hutchinson Technology, Hutchinson, Minnesota, USA) and 25 mm-probe attached to the thenar eminence of the right hand. The thenar eminence is an anatomical region with no subcutaneous fat layer, thus providing VOT-parameters highly consistent among subjects.<sup>15,16</sup> When tissue oxygen saturation ( $StO_2$ ) values remained stable for three minutes, a VOT was performed. Baseline, minimal and maximal  $StO_2$  (respectively  $StO_{2\text{basal}}$ ,  $StO_{2\text{min}}$ ,  $StO_{2\text{max}}$ ), total haemoglobin index before ( $THI_{\text{basal}}$ ) and during VOT ( $THI_{\text{occlu}}$ ),  $StO_2$  descending (desc) and ascending (asc) slopes, time to  $StO_{2\text{max}}$  ( $Time_{\text{max}}$ ), time to baseline ( $Time_{\text{base}}$ ), and area under the curve of hyperaemia (AUC) were computed (Figure 2). Muscle oxygen consumption ( $VO_2$ ) was calculated according to the following formula:  $NIRS\ VO_2 = (THI_{\text{basal}} + THI_{\text{occlu}}) /$

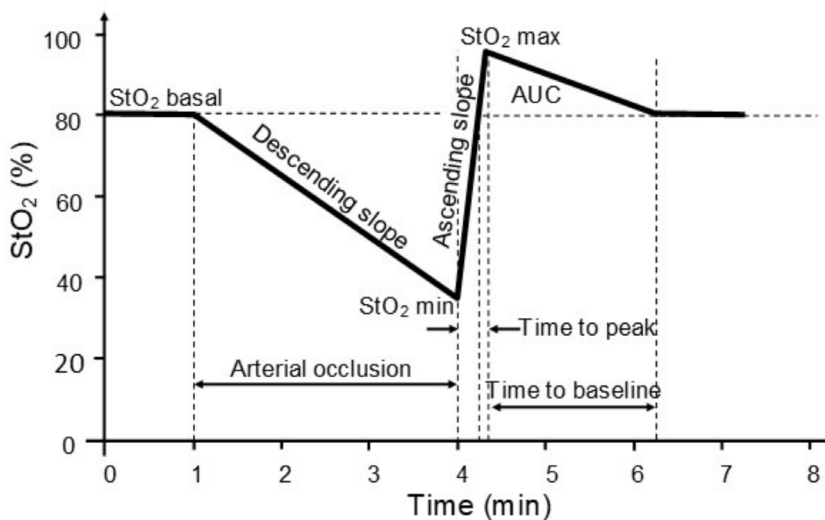
**Figure 1**

Illustration of the study protocol showing the five consecutive conditions (normobaric normoxia, hyperbaric normoxia, hyperbaric hyperoxia, normobaric hyperoxia and normobaric normoxia); near infrared spectroscopy (NIRS), laser Doppler, echocardiography measurements were taken after 30 min of exposure in each condition



**Figure 2**

Schematic representation of tissue oxygen saturation ( $StO_2$ ) evolution during near infrared spectroscopy monitoring of a vascular occlusion test; AUC – area under curve



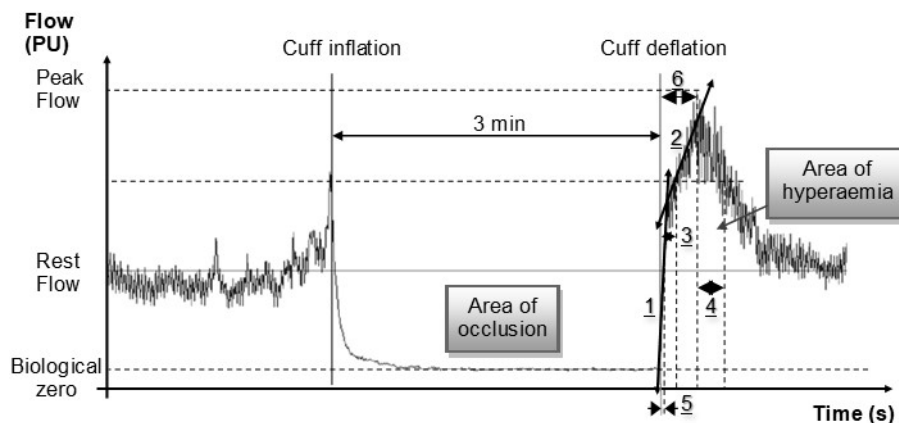
$2 \times (-Desc\ slope)$ .<sup>17</sup> Tissue oxygen saturation variations during ( $\Delta StO_{2min}$ ) and after ( $\Delta StO_{2max}$ ) VOT were also calculated. Schematically,  $StO_{2max}$  and AUC represent oxygen delivery;  $Time_{base}$ ,  $Time_{max}$ , Asc slope and  $\Delta StO_{2max}$  explore microvascular reactivity;  $\Delta StO_{2min}$  reflects the extent of ischaemia and is known to influence Asc slope.<sup>15</sup>

Laser Doppler flowmetry recorded cutaneous blood flow (expressed in perfusion units [PU]) continuously throughout the procedure by using the laser Doppler shift principle to measure velocity and concentration of moving blood cells. The laser Doppler flowmeter probe (PERIFLUX® PF407 (Perimed, Jirfalla, Sweden) was placed on the right index fingertip. The gain was adjusted to 1, the cut-off frequency to 12 Hz, and the time constant to 0.2 seconds.

Recordings were later analysed with Perisoft for Windows 2.5.5 software. Microvascular reactivity was tested with VOTs. The signal obtained during arterial occlusion is flux-independent and was taken as biological zero (BZ). Rest flow (RF) was measured during the 5 min before VOT. The first ascending slope (Slope 1), a reflection of the myogenic phase of hyperaemia, was measured during the first 3 s of the hyperaemic peak. Given that peak flow (PF) occurred later than 3 s, a second ascending slope (Slope 2), a reflection of the hyperaemia metabolic phase, was measured during the interval between the end of the first 3 s and peak flow.<sup>18</sup> Parameters exploring microvascular reactivity including time to recovery (TR), time to half of the difference between rest and peak flow during onset of hyperaemia (TH1), time to half of the difference between rest and peak flow during

**Figure 3**

Example of a laser Doppler recording during post-occlusion hyperaemia; 1 – first upward slope; 2 – second upward slope; 3 – time to half of the difference between rest and peak flow during onset of hyperaemia; 4 – time to half of the difference between rest and peak flow during offset of hyperaemia; 5 – time to recovery; 6 – time to max; PU – perfusion units



offset of hyperaemia (TH2), time to max (TM), and the ratio of the hyperaemia area over the occlusion area (AH/AO), were also computed (Figure 3).<sup>19</sup>

#### Haemodynamic parameters

Non-invasive monitoring (heart rate, arterial pressure) was obtained with a HAUX-MEDICAL-MONITORING® system (Haux-Life-Support GmbH, Karlsbad-Ittersbach, Germany). Systolic arterial pressure – heart rate product (SAP\*HR) was calculated as a reflection of myocardial oxygen consumption.<sup>20</sup>

Transthoracic echocardiography (TTE) was performed with a VIVID-I® echocardiograph (GE Medical Systems, Milwaukee, WI, USA). The left ventricle was studied via volumetric analyses (left ventricular end-diastolic volume [LVEDV], left ventricular end-systolic volume [LVESV]), systolic function parameters (left ventricular ejection fraction [LVEF] [modified Simpson method], subaortic velocity-time integral [AoVTI]) and diastolic function parameters (mitral inflow doppler assessment including E- and A-wave velocity [respectively E and A] and E-wave deceleration time [EDT], tissue Doppler of the mitral annulus e'-wave [e]). The right ventricle function was assessed through tricuspid annular plane systolic excursion (TAPSE) and tissue Doppler of the tricuspid annulus S-wave (S). We then calculated E/A and E/e ratios, left ventricle stroke volume (SV-TTE) and cardiac output (CO-TTE). We used the left ventricular outflow tract Doppler method as it has been previously validated and has shown an acceptable agreement with the thermodilution method.<sup>21</sup> A single investigator, qualified in transthoracic echocardiography performed all measurements. To reduce intra-observer variability the average of three measures was used.

#### STATISTICAL ANALYSIS

Statistical analysis was performed using GraphPad PRISM® (version 8.2.0, GraphPad Software, San Diego, CA, USA). Categorical variables were expressed as frequencies with percentages. Continuous variables with a normal distribution were expressed as mean (standard deviation); otherwise, data were presented as medians with percentiles [25; 75%]. For comparison at different times, a one-way analysis of variance (ANOVA) or Friedman's test was used as appropriate with Tukey's corrections for repeated measurements. A two-sided  $P < 0.05$  was considered as significant.

#### Results

Fifteen subjects were included; three (20%) females and 12 (80%) males, aged 48.4 (SD 11.1) years, with an average height and weight of 1.75 (0.08) m and 75.5 (7.7) kg respectively, representing a mean body mass index of 24.8 (2.5) kg·m<sup>-2</sup>.

There was no statistical difference between the beginning and end normobaric normoxia conditions (i.e., T0 vs T4) in either microcirculatory or haemodynamic measurements.

Haemodynamic data are presented in Table 1. Briefly, two significant changes occurred in hyperoxic conditions (i.e., T2 and T3); bradycardia and a rise in arterial pressure. They both reached a maximum with HB hyperoxia (T2). Of note, bradycardia also occurred during hyperbaric normoxia (T1). There were no changes in echocardiographic measurements in any conditions.

Microcirculatory data gathered with NIRS and laser-Doppler flowmetry are presented in Table 2 and Table 3 respectively.

**Table 1**

Haemodynamic changes ( $n = 15$ ); data are mean (standard deviation); a –  $P < 0.05$  vs baseline; b –  $P < 0.05$  vs hyperbaric normoxia; c –  $P < 0.05$  vs hyperbaric hyperoxia; d –  $P < 0.05$  vs normobaric hyperoxia; e –  $P < 0.05$  vs normobaric normoxia; HR\*SAP – index of myocardial oxygen consumption; LVEDV – left ventricle end-diastolic volume; LVEF\_SBP – modified Simpson method left ventricle ejection fraction; LVESV – left ventricle end-systolic volume; MA e-wave velocity – mitral annulus e-wave velocity; SV\_VTI – stroke volume calculated with velocity-time integral of the left ventricular outflow track; VTI – velocity-time integral of the left ventricular outflow track; TAPSE – tricuspid annular plane systolic excursion; TA S-wave velocity – tricuspid annulus S-wave velocity

Condition	Normobaric normoxia	Hyperbaric normoxia	Hyperbaric hyperoxia	Normobaric hyperoxia	Normobaric normoxia
<b>Haemodynamic monitoring</b>					
Heart rate (beats·min <sup>-1</sup> )	66 (8) <sup>b,c,d</sup>	61 (8) <sup>a,c</sup>	55 (7) <sup>a,b,d,e</sup>	60 (10) <sup>a,b</sup>	62 (8) <sup>c</sup>
Systolic arterial pressure (mmHg)	127 (14) <sup>c,d</sup>	132 (13)	136 (12) <sup>a</sup>	135 (19) <sup>a</sup>	130 (11)
Mean arterial pressure (mmHg)	95 (11) <sup>c</sup>	99 (8)	105 (12) <sup>a,e</sup>	100 (8)	98 (8) <sup>c</sup>
Diastolic arterial pressure (mmHg)	79 (8) <sup>c</sup>	79 (8) <sup>c</sup>	89 (8) <sup>a,b,d,e</sup>	85 (9) <sup>c</sup>	81 (8) <sup>c</sup>
HR*SAP (beats·min <sup>-1</sup> ·mmHg)	8,167 (1,250)	8,162 (1,613)	7,490 (1,208)	8,073 (1,282)	8,150 (1,381)
<b>Transthoracic echocardiography</b>					
LVEDV (mL)	144 (18)	144 (23)	137 (18)	143 (23)	141 (28)
LVESV (mL)	67 (13)	67 (14)	66 (13)	63 (14)	62 (16)
LVEF_SBP (%)	54 (4)	54 (4)	53 (5)	55 (5)	56 (6)
SV_VTI (mL)	69 (10)	70 (14)	72 (15)	71 (15)	68 (14)
VTI (cm)	19 (3)	19 (3)	19 (3)	19 (3)	18 (3)
TAPSE (mm)	23 (4)	24 (3)	21 (3)	21 (3)	23 (3)
TA S-wave velocity (cm·s <sup>-1</sup> )	13 (1)	13 (1)	12 (1)	12 (1)	13 (1)
Mitral E-wave velocity (cm·s <sup>-1</sup> )	63 (12)	64 (13)	62 (8)	61 (8)	60 (12)
E-wave deceleration time (ms)	165 (37)	177 (44)	170 (34)	176 (34)	176 (46)
Mitral A-wave velocity (cm·s <sup>-1</sup> )	50 (11)	51 (13)	47 (12)	50 (9)	48 (9)
MA e-wave velocity (cm·s <sup>-1</sup> )	14 (3)	14 (4)	13 (2)	12 (3)	13 (3)
E/A ratio	1.32 (0.33)	1.36 (0.58)	1.42 (0.40)	1.28 (0.34)	1.27 (0.34)
E/e ratio	4.72 (1.03)	5.11 (1.76)	5.00 (1.02)	5.46 (1.44)	4.84 (1.24)
Cardiac output (L·min <sup>-1</sup> )	4.43 (0.76)	4.33 (0.96)	3.95 (0.83)	4.13 (1.08)	4.20 (0.96)

At rest, there was a significant decrease in perfusion (RF) associated with a significant rise in  $StO_{2\text{basal}}$  during HB hyperoxia. Transcutaneous measurements showed no statistical difference in  $PtcCO_2$  in any conditions. In contrast,  $PtcO_2$  reached a median of 19.1 kPa [16.7; 21.2] in NB hyperoxia and 99.3 kPa [77.3; 137.3] in HB hyperoxia ( $P < 0.0001$  vs T0, T1, T3 and T4) (Figure 4A).

During the ischaemic period, occlusion area ( $P < 0.05$  vs T0, T1 and T4),  $StO_{2\text{min}}$  ( $P < 0.05$  vs T0, T1, T3 and T4) and  $\Delta StO_{2\text{min}}$  ( $P < 0.05$  vs T0, T1 and T4) were significantly lower in HB hyperoxia. In parallel, laser-Doppler PORH parameters (peak flow, hyperaemia area and Slope 1) decreased significantly during HB hyperoxia (Figure 4B).

No parameters relating to microvascular reactivity (i.e., ascending slope, TR,  $\Delta StO_{2\text{max}}$ , RF/PF and AH/AO ratios) showed any significant changes at any time of the experiment (Figure 4C).

## Discussion

This study confirmed previously published effects of normobaric hyperoxia on the microcirculation in healthy volunteers.<sup>7</sup> By increasing the oxygen dose, hyperbaric hyperoxia further increases the magnitude of these effects. Of note, microvascular reactivity remained unimpaired throughout the protocol, suggesting that these alterations are indeed an adaptative phenomenon.

**Table 2**

Near infrared spectroscopy variables ( $n = 15$ ); data are mean (standard deviation) or median [25;75% percentiles]; a –  $P < 0.05$  vs baseline; b –  $P < 0.05$  vs hyperbaric normoxia; c –  $P < 0.05$  vs hyperbaric hyperoxia; d –  $P < 0.05$  vs normobaric hyperoxia; e –  $P < 0.05$  vs normobaric normoxia; AU – arbitrary unit; AUC – area under curve of hyperaemia; NIRS  $VO_2$  – muscle oxygen consumption;  $StO_2$  – tissue oxygen saturation;  $\Delta StO_{2max}$  – calculated from  $(StO_{2max} - StO_{2basal})/StO_{2basal}$ ;  $\Delta StO_{2min}$  – calculated from  $(StO_{2min} - StO_{2basal})/StO_{2basal}$ ; THI – total haemoglobin index

Condition	Normobaric normoxia	Hyperbaric normoxia	Hyperbaric hyperoxia	Normobaric hyperoxia	Normobaric normoxia
$StO_{2basal}$ (%)	81 (3) <sup>c</sup>	81 (2) <sup>c</sup>	85 (4) <sup>a,b,d,e</sup>	81 (3) <sup>c</sup>	80 (3) <sup>c</sup>
$StO_{2min}$ (%)	52 (7) <sup>c</sup>	52 (6) <sup>c,d</sup>	62 (8) <sup>a,b,d,e</sup>	56 (4) <sup>b,c</sup>	51 (5) <sup>c</sup>
$StO_{2max}$ (%)	95 [93; 97] <sup>c</sup>	96 [94; 97] <sup>c</sup>	99 [97; 99] <sup>a,b,e</sup>	96 [96; 99] <sup>c,e</sup>	94 [91; 96] <sup>c,d</sup>
$\Delta StO_{2max}$ (%)	17 (3)	18 (3)	15 (4)	19 (5)	17 (6)
$\Delta StO_{2min}$ (%)	-38 [-43; -29] <sup>c</sup>	-36 [-41; -33] <sup>c</sup>	-28 [-35; -18] <sup>a,b,e</sup>	-32 [-35; -28]	-35 [-39; -32] <sup>c</sup>
THI <sub>basal</sub> (AU)	15.4 (2.3) <sup>c,d</sup>	14.4 (2.2)	13.8 (2.7) <sup>a</sup>	13.7 (2.4) <sup>a</sup>	14.5 (2.0)
THI <sub>occlu</sub> (AU)	15.3 (3.1) <sup>c</sup>	14.7 (2.9) <sup>c</sup>	13.0 (3.2) <sup>a,b</sup>	14.2 (2.7)	14.6 (1.9)
Descending slope (%·s <sup>-1</sup> )	-0.15 (0.03) <sup>c</sup>	-0.15 (0.03)	-0.13 (0.04) <sup>a</sup>	-0.14 (0.03)	-0.15 (0.04)
Ascending slope (%·s <sup>-1</sup> )	2.53 [1.69; 6.81]	5.67 [2.79; 8.25]	2.42 [1.71; 4.33]	2.17 [1.65; 4.75]	2.82 [1.6; 5.16]
Time <sub>max</sub> (s)	29 (11)	26 (8)	32 (10)	37 (15)	33 (15)
Time <sub>base</sub> (s)	277 [222; 353]	256 [201; 332]	388 [235; 457]	325 [166; 436]	277 [138; 353]
AUC (%·s)	1,475 (617) <sup>c</sup>	1,706 (737)	2,414 (1,143) <sup>a</sup>	2,161 (1,262)	1,680 (1,107)
NIRS $VO_2$ (AU)	2.32 (0.58) <sup>c</sup>	2.19 (0.58) <sup>c,d</sup>	1.69 (0.68) <sup>a,b,e</sup>	1.94 (0.55) <sup>b</sup>	2.23 (0.63) <sup>c</sup>

## HAEMODYNAMIC CHANGES

Haemodynamic change was investigated as interactions with the microcirculation have been previously described.<sup>22</sup> This phenomenon is known as haemodynamic coherence. It stipulates that hemodynamic alterations have a direct effect on regional and microcirculatory perfusion and oxygen delivery to the cells.

Hyperoxia-induced bradycardia is a well-known phenomenon described for the first time in 1897 and proven by others.<sup>23</sup> In that study, HBO induced a more significant bradycardia than normobaric hyperoxia (a reduction of 12–16 beats·min<sup>-1</sup> vs 4–7 beats·min<sup>-1</sup>). Both oxygen-dependent (a direct effect of high oxygen tension on myocardium<sup>24</sup> and autonomic nervous system alterations<sup>25,26</sup>) and oxygen-independent mechanisms (diminution in sympathetic tone) were involved in the phenomenon. Bradycardia is known to reach a maximum under therapeutic barometric pressure ranges and to gradually disappear over time.<sup>27</sup>

In our study, HBO induced a hyperoxic vasoconstriction, and as a consequence, a rise of approximately 10 mmHg in systolic, diastolic and mean arterial blood pressures. This phenomenon occurs in healthy small diameter arterioles as soon as the  $PO_2$  reaches 101.3 kPa.<sup>28</sup> A further increase

in  $PO_2$  (up to 202.7 kPa<sup>29</sup>) constricts larger vessels such as resistance arteries, leading to a rapid rise in systemic vascular resistance,<sup>30</sup> hence in arterial blood pressure.

As arterial hypertension originated from microcirculatory modifications (e.g., hyperoxic vasoconstriction) while cardiac output remained steady, haemodynamic changes did not impact the microcirculation. Hence, all microcirculatory modifications may be considered a direct consequence of the oxygen exposure.

## MICROCIRCULATORY CHANGES

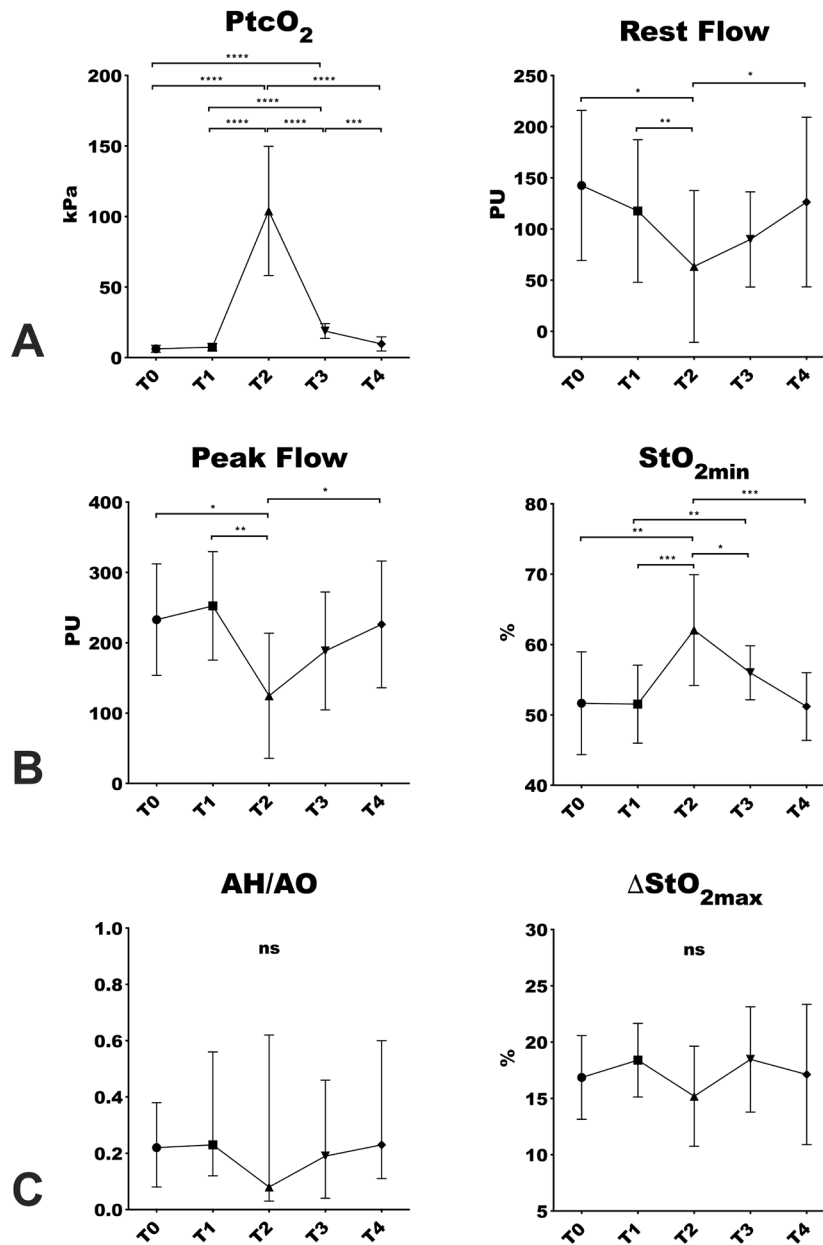
This study showed that significant microcirculatory modifications occur during normobaric and hyperbaric hyperoxia. In comparison with baseline value,  $PtcO_2$  increased during normobaric hyperoxia (18.8 [SD 5.2] vs 6.1 [2.4] kPa). In response, a fall in rest flow occurred (Figure 4A). Even though it does not reach statistical significance, probably due to insufficient number of subjects, these results are consistent with previously published data.<sup>7,31</sup> Hyperbaric oxygen, by leading to a critical rise in  $PtcO_2$  (104.0 [45.9] kPa) significantly reduced microcirculatory flow. As hyperbaric normoxia has no effects on the microcirculation, it seems that the high oxygen pressure drives this phenomenon.

**Table 3**  
 Laser-Doppler flowmetry variables ( $n = 15$ ); data are mean (standard deviation) or median [25; 75% percentiles]; a –  $P < 0.05$  vs baseline; b –  $P < 0.05$  vs hyperbaric normoxia; c –  $P < 0.05$  vs hyperbaric hyperoxia; d –  $P < 0.05$  vs normobaric hyperoxia; e –  $P < 0.05$  vs normobaric normoxia; AH/AO – hyperaemia area / occlusion area ratio; AU – arbitrary unit; PF – peak flow; PU – perfusion units; RF – rest flow;  $\Delta$ RF\_PF – calculated from ((peak flow – rest flow) / rest flow) x 100

Condition	Normobaric normoxia	Hyperbaric normoxia	Hyperbaric hyperoxia	Normobaric hyperoxia	Normobaric normoxia
Rest flow (PU)	143 (73) <sup>c</sup>	118 (70) <sup>c</sup>	63 (74) <sup>a,b,e</sup>	90 (47)	126 (83) <sup>c</sup>
Peak flow (PU)	233 (79) <sup>c</sup>	253 (77) <sup>c</sup>	125 (89) <sup>a,b,e</sup>	188 (84)	226 (90) <sup>c</sup>
$\Delta$ RF_PF (%)	72 [31; 173]	127 [59; 172]	93 [49; 274]	154 [47; 218]	111 [59; 191]
Occlusion area (PU.s)	24,602 [16,808; 37,431] <sup>c</sup>	19,821 [13,007; 29,987] <sup>c</sup>	7,387 [5,524; 13,917] <sup>a,b,e</sup>	18,747 [7,553; 23,675]	19,700 [9,986; 59,397] <sup>c</sup>
Hyperaemia area (PU.s)	4,442 [1,800; 8,249] <sup>c</sup>	4,237 [2,948; 7,467] <sup>c</sup>	0,519 [0,311; 1,678] <sup>a,b,e</sup>	1,920 [0,802; 6,701]	6,923 [4,145; 10,488] <sup>c</sup>
AH/AO ratio	0.22 [0.08; 0.38]	0.23 [0.12; 0.56]	0.08 [0.03; 0.62]	0.19 [0.04; 0.46]	0.23 [0.11; 0.60]
Time to recovery (s)	1.12 [0.96; 1.32]	0.97 [0.56; 1.52]	1.65 [0.73; 3.29]	1.05 [0.40; 1.95]	1.24 [0.53; 1.60]
Time to half before hyperaemia (s)	0.95 [0.71; 1.76]	1.02 [0.71; 4.82] <sup>c</sup>	3.13 [1.18; 9.65] <sup>b</sup>	1.08 [0.62; 4.40]	0.93 [0.71; 1.84]
Time to max (s)	39.75 (59.42)	25.62 (14.94)	41.24 (49.26)	14.53 (12.07)	36.00 (24.00)
Time to half after hyperaemia (s)	34.15 [13.95; 82.53]	42.44 [27.53; 53.81]	26.32 [8.31; 73.13]	27.93 [13.55; 41.17] <sup>e</sup>	59.67 [42.84; 71.49] <sup>d</sup>
Slope 1 (PU.s <sup>-1</sup> )	58.4 [38.0; 79.1] <sup>c</sup>	52.5 [33.9; 89.1] <sup>c</sup>	19.5 [10.1; 35.1] <sup>a,b</sup>	47.7 [28.0; 77.0]	56.7 [32.0; 68.6]
Slope 2 (PU.s <sup>-1</sup> )	5.3 [4.2; 7.3]	3.6 [2.8; 4.9]	4.3 [0.9; 5.0]	5.3 [4.6; 9.2]	2.7 [1.5; 5.5]

Figure 4

A – microcirculatory parameters at rest; B – results of ischaemic stimulus and vascular reserve mobilisation; C – microvascular reactivity; \* $P < 0.05$ ; \*\* $P < 0.01$ ; \*\*\* $P < 0.001$ ; \*\*\*\* $P < 0.0001$ ; AH/AO – hyperaemic area / occlusion area ratio; ns – not significant;  $PtcO_2$  – transcutaneous partial pressure of oxygen; PU – perfusion units;  $StO_2$  – tissue oxygen saturation measured with near infrared spectroscopy;  $\Delta StO_{2max}$  – calculated from  $(StO_{2max} - StO_{2basal})/StO_{2basal}$ ; T0 – baseline normobaric normoxia; T1 – hyperbaric normoxia; T2 – hyperbaric hyperoxia; T3 – normobaric hyperoxia; T4 – final normobaric normoxia



The underlying mechanism highlighted is known as hyperoxic vasoconstriction.<sup>29,32</sup> It is an adaptative response to protect cellular integrity from high oxygen tension.<sup>33,34</sup> The mechanisms by which hyperoxia leads to systemic vasoconstriction are not fully elucidated. The elevated arterial content of oxygen ( $CaO_2$ ) itself may contribute due to the pivotal role of the erythrocyte. Following a fall in haemoglobin- $O_2$  saturation, haemoglobin may act as an ‘ $O_2$  sensor’, releasing adenosine triphosphate (ATP) and nitric

oxide. Conversely, plasma ATP concentrations are lower in hyperoxia, suggesting reduced vasodilator signalling. Moreover, the high  $PaO_2$  may reduce the availability of other vasodilators such as prostaglandin  $PGI_2$ .<sup>35</sup> Finally, hyperoxia causes an increase in reactive oxygen species (ROS), which in turn inhibit a range of vasodilators such as nitric oxide (e.g., superoxide reacts with nitric oxide to generate peroxynitrite).<sup>13</sup> Then, during prolonged HBO exposure, the activation of extracellular superoxide

dismutase removes superoxide and reduces nitric oxide antagonism. Thus, the hyperoxic vasoconstriction could be transient as recently reported elsewhere.<sup>13</sup>

Previous studies have proved that hyperoxic vasoconstriction only takes place in well-perfused territories while microvascular flow remains stable in ischaemic tissues.<sup>31</sup> It should result in microvascular flow redistribution toward poorly perfused territories. This phenomenon, known as the 'Robin-Hood effect', is supportive of the use of HBO in patients with heterogeneous microcirculation alterations such as ischaemia-reperfusion injuries.<sup>31</sup>

Performing VOTs in our study allowed us to explore vascular reserve, and the integrity and functionality of the microcirculation when exposed to elevated  $PO_2$ . Parameters exploring microvascular reactivity (i.e., NIRS Time<sub>base</sub>, Time<sub>max</sub>, Asc slope and  $\Delta StO_{2max}$ ; and laser-Doppler AH/AO and RF/PF ratios) do not vary over time (Figure 4C). One study had already demonstrated similar results under normobaric hyperoxia.<sup>7</sup> Our study extends their findings to higher oxygen pressures. It emphasises the fact that hyperoxic vasoconstriction is an adaptative phenomenon that does not alter microvascular reactivity.

Laser Doppler parameters exploring vascular reserve (i.e., PF, Slope 1 and AH) decrease significantly under hyperbaric hyperoxia. However, the ischaemic stimulus (i.e.,  $StO_{2min}$ ,  $\Delta StO_{2min}$  and occlusion area) is substantially lower during hyperbaric hyperoxia (Figure 4B). The predefined 3-min period of ischaemia produces a weaker ischaemic stimulus, probably because  $StO_{2basal}$  is higher and dissolved oxygen must first be consumed before tissues react to hypoxia.<sup>7</sup> Hence, a smaller part of the available vascular reserve is mobilised in response to ischaemia.

In parallel,  $StO_{2max}$  and AUC significantly increase. These phenomena also occur during normobaric hyperoxia (without reaching statistical significance) but are absent during hyperbaric normoxia. This highlights the fact that the rise in arterial oxygen content plays a decisive part in these modifications.

A marked but statistically non-significant drop in TH2 (20%) suggests a faster vascular reserve demobilisation during normobaric and hyperbaric hyperoxia. The rise in oxygen delivery (represented by  $StO_{2max}$  and AUC) may have triggered protective mechanisms to limit the PORH duration. Further studies are needed to confirm or refute this hypothesis.

In our study, the reduction in  $StO_2$  Desc slope and NIRS  $VO_2$  during normobaric hyperoxia and hyperbaric hyperoxia raise important methodological issues. First, in hyperoxic conditions, the dissolved oxygen rises. In hyperbaric hyperoxia, it could reach up to 6 mL·100 mL<sup>-1</sup> of plasma at 304.0 kPa. This amount is sufficient to cover all biological

needs.<sup>36</sup> Hence, during VOT, this supplement in dissolved oxygen (which can't be detected by NIRS- $StO_2$ ) must be consumed before the signal starts to decrease. This time-lapse between cuff inflation and the inflection point of the Desc slope alters the reliability of these parameters. Then, when multiple VOTs are repeated, a phenomenon called ischaemic preconditioning occurs. As highlighted in a previous study, ischaemic preconditioning results in a drop in Desc slope.<sup>37</sup> Thus, Desc slope and NIRS  $VO_2$  interpretations in our study may be unreliable. Future studies would have to focus on oxygen-induced changes on a metabolic level to further investigate this phenomenon.

## LIMITATIONS

Our study has several limitations. First, the small number of healthy volunteers limits the study power and its capacity to detect slight variations or different response patterns. Hence, the effect of age or gender on microcirculatory response to hyperoxia could not be investigated. Moreover, we excluded patients > 65 years, whereas many of the patients treated with HBO are > 65 years. This may limit the generalisability of our results. Second, the sex ratio, largely in favour of men (80% vs 20%) limits a wider application of our findings to the general population as gender is known to impact microcirculatory measurements. Third, we standardised the extent of the ischaemic insult with a predefined three minute ischaemic period. Alternatively, we could have used a predefined  $StO_2$  threshold (as proposed by Bezemer et al.<sup>15</sup>) to release cuff inflation. Doing so, VOTs would have taken more than three minutes and might have become uncomfortable for healthy awake subjects.

Finally, our study was designed to explore oxygen-induced microcirculation alterations but is limited in its ability to explore their pathophysiological mechanisms. We decided to be as non-invasive as possible to make recruitment of volunteers easier. Nevertheless, invasive blood flow and  $VO_2$  measurements, blood samples to investigate inflammatory pathways, or *in vivo* microdialysis may be of interest to further investigate this question.

## Conclusions

High oxygen tensions significantly alter haemodynamics and microcirculation in healthy subjects, with hyperbaric oxygen exposure further increasing those modifications. Bradycardia occurred while cardiac output remained constant and arterial blood pressure increased. The rise in tissue oxygen saturation and transcutaneous oxygen partial pressure promotes an adaptative vasoconstrictive response to protect cellular integrity. Indeed, microvascular reactivity remained unaltered and vascular reserve is mobilised in proportion to the magnitude of an ischaemic stimulus. Further experiments are required to understand the pathophysiological pathways involved in hyperoxia-induced microcirculation modifications and to explore its effects in pathological conditions such as ischaemia or sepsis.

## References

- 1 Damiani E, Adrario E, Girardis M, Romano R, Pelaia P, Singer M, et al. Arterial hyperoxia and mortality in critically ill patients: a systematic review and meta-analysis. *Crit Care*. 2014;18(6):711. doi: [10.1186/s13054-014-0711-x](https://doi.org/10.1186/s13054-014-0711-x). PMID: [25532567](https://pubmed.ncbi.nlm.nih.gov/25532567/). PMCID: [PMC4298955](https://pubmed.ncbi.nlm.nih.gov/PMC4298955/).
- 2 Helmerhorst HJF, Roos-blom MJ, van Westerloo DJ, de Jonge E. Association between arterial hyperoxia and outcome in subsets of critical illness: a systematic review, meta-analysis, and meta-regression of cohort studies. *Crit Care Med*. 2015;43:1508–19. doi: [10.1097/CCM.0000000000000998](https://doi.org/10.1097/CCM.0000000000000998). PMID: [25855899](https://pubmed.ncbi.nlm.nih.gov/25855899/).
- 3 Waisman D, Brod V, Rahat MA, Amit-Cohen B-C, Lahat N, Rimar D, et al. Dose-related effects of hyperoxia on the lung inflammatory response in septic rats. *Shock*. 2012;37:95–102. doi: [10.1097/SHK.0b013e3182356fc3](https://doi.org/10.1097/SHK.0b013e3182356fc3). PMID: [21921827](https://pubmed.ncbi.nlm.nih.gov/21921827/).
- 4 Sun L, Strelow H, Mies G, Veltkamp R. Oxygen therapy improves energy metabolism in focal cerebral ischemia. *Brain Res*. 2011;1415:103–8. doi: [10.1016/j.brainres.2011.07.064](https://doi.org/10.1016/j.brainres.2011.07.064). PMID: [21872850](https://pubmed.ncbi.nlm.nih.gov/21872850/).
- 5 Veltkamp R, Siebing DA, Sun L, Heiland S, Bieber K, Marti HH, et al. Hyperbaric oxygen reduces blood–brain barrier damage and edema after transient focal cerebral ischemia. *Stroke*. 2005;36:1679–83. doi: [10.1161/01.STR.0000173408.94728.79](https://doi.org/10.1161/01.STR.0000173408.94728.79). PMID: [16020761](https://pubmed.ncbi.nlm.nih.gov/16020761/).
- 6 Mathieu D, Marroni A, Kot J. Tenth European consensus conference on hyperbaric medicine: recommendations for accepted and non-accepted clinical indications and practice of hyperbaric oxygen treatment. *Diving Hyperb Med*. 2017;47:24–32. doi: [10.28920/dhm47.1.24-32](https://doi.org/10.28920/dhm47.1.24-32). PMID: [28357821](https://pubmed.ncbi.nlm.nih.gov/28357821/). PMCID: [PMC6147240](https://pubmed.ncbi.nlm.nih.gov/PMC6147240/).
- 7 Orbegozo Cortés D, Puflea F, Donadello K, Taccone FS, Gottin L, Creteur J, et al. Normobaric hyperoxia alters the microcirculation in healthy volunteers. *Microvasc Res*. 2015;98:23–8. doi: [10.1016/j.mvr.2014.11.006](https://doi.org/10.1016/j.mvr.2014.11.006). PMID: [25433297](https://pubmed.ncbi.nlm.nih.gov/25433297/).
- 8 Sakr Y, Dubois MJ, De Backer D, Creteur J, Vincent JL. Persistent microcirculatory alterations are associated with organ failure and death in patients with septic shock. *Crit Care Med*. 2004;32:1825–31. doi: [10.1097/01.ccm.0000138558.16257.3f](https://doi.org/10.1097/01.ccm.0000138558.16257.3f). PMID: [15343008](https://pubmed.ncbi.nlm.nih.gov/15343008/).
- 9 Weglicki WB, Whalen RE, Thompson HK, McIntosh HD. Effects of hyperbaric oxygenation on excess lactate production in exercising dogs. *Am J Physiol*. 1966;210:473–7. doi: [10.1152/ajplegacy.1966.210.3.473](https://doi.org/10.1152/ajplegacy.1966.210.3.473). PMID: [5933195](https://pubmed.ncbi.nlm.nih.gov/5933195/).
- 10 Stellingwerff T, Glazier L, Watt MJ, LeBlanc PJ, Heigenhauser GJF, Spriet LL. Effects of hyperoxia on skeletal muscle carbohydrate metabolism during transient and steady-state exercise. *J Appl Physiol* (1985). 2005;98:250–6. doi: [10.1152/jappphysiol.00897.2004](https://doi.org/10.1152/jappphysiol.00897.2004). PMID: [15377650](https://pubmed.ncbi.nlm.nih.gov/15377650/).
- 11 Stellingwerff T, LeBlanc PJ, Hollidge MG, Heigenhauser GJF, Spriet LL. Hyperoxia decreases muscle glycogenolysis, lactate production, and lactate efflux during steady-state exercise. *Am J Physiol Endocrinol Metab*. 2006;290:E1180–90. doi: [10.1152/ajpendo.00499.2005](https://doi.org/10.1152/ajpendo.00499.2005). PMID: [16403777](https://pubmed.ncbi.nlm.nih.gov/16403777/).
- 12 Milstein DMJ, Helmers R, Hackmann S, Belterman CNW, van Hulst RA, de Lange J. Sublingual microvascular perfusion is altered during normobaric and hyperbaric hyperoxia. *Microvasc Res*. 2016;105:93–102. doi: [10.1016/j.mvr.2016.02.001](https://doi.org/10.1016/j.mvr.2016.02.001). PMID: [26851620](https://pubmed.ncbi.nlm.nih.gov/26851620/).
- 13 Yamamoto N, Takada, R, Maeda T, Yoshii T, Okawa A, Yagishita K. Microcirculation and tissue oxygenation in the head and limbs during hyperbaric oxygen treatment. *Diving Hyperb Med*. 2021;51:338–44. doi: [10.28920/dhm51.4.338-344](https://doi.org/10.28920/dhm51.4.338-344). PMID: [34897598](https://pubmed.ncbi.nlm.nih.gov/34897598/). PMCID: [PMC8920905](https://pubmed.ncbi.nlm.nih.gov/PMC8920905/).
- 14 Tee GBY, Rasool AHG, Halim AS, Rahman ARA. Dependence of human forearm skin postocclusive reactive hyperemia on occlusion time. *J Pharmacol Toxicol Methods*. 2004;50:73–8. doi: [10.1016/j.vascn.2004.02.002](https://doi.org/10.1016/j.vascn.2004.02.002). PMID: [15233971](https://pubmed.ncbi.nlm.nih.gov/15233971/).
- 15 Bezemer R, Lima A, Myers D, Klijn E, Heger M, Goedhart PT, et al. Assessment of tissue oxygen saturation during a vascular occlusion test using near-infrared spectroscopy: the role of probe spacing and measurement site studied in healthy volunteers. *Crit Care*. 2009;13:S4. doi: [10.1186/cc8002](https://doi.org/10.1186/cc8002). PMID: [19951388](https://pubmed.ncbi.nlm.nih.gov/19951388/). PMCID: [PMC2786106](https://pubmed.ncbi.nlm.nih.gov/PMC2786106/).
- 16 Gómez H, Mesquida J, Simon P, Kim HK, Puyana JC, Ince C, et al. Characterization of tissue oxygen saturation and the vascular occlusion test: influence of measurement sites, probe sizes and deflation thresholds. *Crit Care*. 2009;13:S3. doi: [10.1186/cc8001](https://doi.org/10.1186/cc8001). PMID: [19951387](https://pubmed.ncbi.nlm.nih.gov/19951387/). PMCID: [PMC2786105](https://pubmed.ncbi.nlm.nih.gov/PMC2786105/).
- 17 Skarda DE, Mulier KE, Myers DE, Taylor JH, Beilman GJ. Dynamic near-infrared spectroscopy measurements in patients with severe sepsis. *Shock*. 2007;27:348–53. doi: [10.1097/01.shk.0000239779.25775.e4](https://doi.org/10.1097/01.shk.0000239779.25775.e4). PMID: [17414414](https://pubmed.ncbi.nlm.nih.gov/17414414/).
- 18 Koller A, Kaley G. Role of endothelium in reactive dilation of skeletal muscle arterioles. *Am J Physiol*. 1990;259:H1313–6. doi: [10.1152/ajpheart.1990.259.5.H1313](https://doi.org/10.1152/ajpheart.1990.259.5.H1313). PMID: [2240236](https://pubmed.ncbi.nlm.nih.gov/2240236/).
- 19 Yvonne-Tee GB, Rasool AHG, Halim AS, Rahman ARA. Reproducibility of different laser Doppler fluximetry parameters of postocclusive reactive hyperemia in human forearm skin. *J Pharmacol Toxicol Methods*. 2005;52:286–92. doi: [10.1016/j.vascn.2004.11.003](https://doi.org/10.1016/j.vascn.2004.11.003). PMID: [16125628](https://pubmed.ncbi.nlm.nih.gov/16125628/).
- 20 Nelson RR, Gobel FL, Jorgensen CR, Wang K, Wang Y, Taylor HL. Hemodynamic predictors of myocardial oxygen consumption during static and dynamic exercise. *Circulation*. 1974;50:1179–89. doi: [10.1161/01.cir.50.6.1179](https://doi.org/10.1161/01.cir.50.6.1179). PMID: [4430113](https://pubmed.ncbi.nlm.nih.gov/4430113/).
- 21 Mercado P, Maizel J, Beyls C, Titeca-Beauport D, Joris M, Kontar L, et al. Transthoracic echocardiography: an accurate and precise method for estimating cardiac output in the critically ill patient. *Crit Care*. 2017;21(1):136. doi: [10.1186/s13054-017-1737-7](https://doi.org/10.1186/s13054-017-1737-7). PMID: [28595621](https://pubmed.ncbi.nlm.nih.gov/28595621/). PMCID: [PMC5465531](https://pubmed.ncbi.nlm.nih.gov/PMC5465531/).
- 22 Ince C. Hemodynamic coherence and the rationale for monitoring the microcirculation. *Crit Care*. 2015;19:S8. doi: [10.1186/cc14726](https://doi.org/10.1186/cc14726). PMID: [26729241](https://pubmed.ncbi.nlm.nih.gov/26729241/).
- 23 Fagraeus L, Hesser CM, Linnarsson D. Cardiorespiratory responses to graded exercise at increased ambient air pressure. *Acta Physiol Scand*. 1974;91:259–74. doi: [10.1111/j.1748-1716.1974.tb05682.x](https://doi.org/10.1111/j.1748-1716.1974.tb05682.x). PMID: [4846323](https://pubmed.ncbi.nlm.nih.gov/4846323/).
- 24 Fagraeus L, Linnarsson D. Heart rate in the hyperbaric environment after autonomic blockade. *Acta Physiol Scand*. 1973;9:260–4.
- 25 Yamazaki F, Wada F, Nagaya K, Torii R, Endo Y, Sagawa S, et al. Autonomic mechanisms of bradycardia during nitrox exposure at 3 atmospheres absolute in humans. *Aviat Space Environ Med*. 2003;74(6 Pt 1):643–8. PMID: [12793536](https://pubmed.ncbi.nlm.nih.gov/12793536/).
- 26 Bergø GW, Risberg J, Tyssebotn I. Effect of 5 bar oxygen on cardiac output and organ blood flow in conscious rats. *Undersea Biomed Res*. 1988;15:457–70. PMID: [3227578](https://pubmed.ncbi.nlm.nih.gov/3227578/).
- 27 Yamazaki F, Shiraki K, Sagawa S, Endo Y, Torii R, Yamaguchi H, et al. Assessment of cardiac autonomic nervous activities during heliox exposure at 24 atm abs. *Aviat Space Environ Med*. 1998;69:643–6. PMID: [9681370](https://pubmed.ncbi.nlm.nih.gov/9681370/).
- 28 Dooley JW, Mehm WJ. Non invasive assessment of the vasoconstrictive effects of hyperoxygenation. *J Hyperb Med*. 1989;4:177–87.

- 29 Sonny M, Sam AD, Piantadosi CA, Klitzman B. Effects of hyperbaric oxygenation on arteriolar diameter in rat cremaster muscle. *Undersea Hyperb Med.* 1993;20:64.
- 30 Granger HJ, Goodman AH, Granger DN. Role of resistance and exchange vessels in local microvascular control of skeletal muscle oxygenation in the dog. *Circ Res.* 1976;38:379–85. doi: [10.1161/01.res.38.5.379](https://doi.org/10.1161/01.res.38.5.379). PMID: [1269076](https://pubmed.ncbi.nlm.nih.gov/1269076/).
- 31 Mathieu D, Nevriere D, Millien JP, Coget JM, Wattel F. Non invasive assessment of vasoconstrictive effects of hyperoxygenation in focal ischaemia. In: Bennett PB, Marquis RE, editors. *Basic and applied high pressure biology*. Rochester: University of Rochester Press; 1994. p. 375–81.
- 32 Sullivan SM, Johnson PC. Effect of oxygen on arteriolar dimensions and blood flow in cat sartorius muscle. *Am J Physiol.* 1981;241:H547–56. doi: [10.1152/ajpheart.1981.241.4.H547](https://doi.org/10.1152/ajpheart.1981.241.4.H547). PMID: [7315979](https://pubmed.ncbi.nlm.nih.gov/7315979/).
- 33 Whalen WJ, Nair P. Intracellular PO<sub>2</sub> and its regulation in resting skeletal muscle of the guinea pig. *Circ Res.* 1967;21:251–61. doi: [10.1161/01.res.21.3.251](https://doi.org/10.1161/01.res.21.3.251). PMID: [6054008](https://pubmed.ncbi.nlm.nih.gov/6054008/).
- 34 Whalen WJ, Nair P. Skeletal muscle PO<sub>2</sub>: effect of inhaled and topically applied O<sub>2</sub> and CO<sub>2</sub>. *Am J Physiol.* 1970;218:973–80. doi: [10.1152/ajplegacy.1970.218.4.973](https://doi.org/10.1152/ajplegacy.1970.218.4.973). PMID: [5435430](https://pubmed.ncbi.nlm.nih.gov/5435430/).
- 35 Brugniaux JV, Coombs GB, Barak OF, Dujic Z, Sekhon MS, Ainslie PN. Highs and lows of hyperoxia: physiological, performance, and clinical aspects. *Am J Physiol Regul Integr Comp Physiol.* 2018;315:R1–R27. doi: [10.1152/ajpregu.00165.2017](https://doi.org/10.1152/ajpregu.00165.2017). PMID: [29488785](https://pubmed.ncbi.nlm.nih.gov/29488785/).
- 36 Lanphier EH, Brown N. The physiological basis of hyperbaric therapy. In: *Fundamentals of hyperbaric medicine by the Committee on Hyperbaric Oxygenation*. Washington DC: National Academy of Sciences National Research Council; 1966. p. 33–55.
- 37 Orbeago Cortés D, Puflea F, De Backer D, Creteur J, Vincent JL. Near infrared spectroscopy (NIRS) to assess the effects of local ischemic preconditioning in the muscle of healthy volunteers and critically ill patients. *Microvasc Res.* 2015;102:25–32. doi: [10.1016/j.mvr.2015.08.002](https://doi.org/10.1016/j.mvr.2015.08.002). PMID: [26265192](https://pubmed.ncbi.nlm.nih.gov/26265192/).

#### Acknowledgments

We would like to thank all volunteers for their participation in the experiment, the Clinical Investigation Centre, and the staff of the Hyperbaric Oxygen Therapy Centre of Lille teaching hospital for their support.

#### Conflicts of interest and funding

This work was supported by CHU Lille. No conflicts of interest were declared.

**Submitted:** 14 April 2022

**Accepted after revision:** 1 October 2022

**Copyright:** This article is the copyright of the authors who grant *Diving and Hyperbaric Medicine* a non-exclusive licence to publish the article in electronic and other forms.



## HBOEvidence pages

Short critical appraisals of all randomised controlled trials and systematic reviews in both diving and hyperbaric medicine. <http://hboevidence.wikis.unsw.edu.au>

Pages written and maintained by The HBOE Working Group. This site is freely available to the public and professionals alike.

We still welcome volunteers to contribute CATs to the site.  
Contact Professor Michael Bennett [m.bennett@unsw.edu.au](mailto:m.bennett@unsw.edu.au) if you are interested.